New battery model for consolidating a health monitoring system model of reusable launcher power harness

Mickaël Cartron, Mariem Slimani, Nicolas Gregis, David Monchaux, Dominique Besson

73rd International Astronautical Congress (IAC), Paris, France, 18-22 September 2022.

IAC-22-22,D2,IP,1,x69418

New battery Model for consolidating a health monitoring system model of reusable launcher power harness

Mickaël Cartron[a*], Mariem Slimani[a], Nicolas Grégis[a], David Monchaux[b], Dominique Besson[b]

[a] Université Paris-Saclay, CEA, List, F-91120, Palaiseau, France,
mickael.cartron@cea.fr, mariem.slimani@cea.fr, nicolas.gregis@cea.fr
[b] Centre National d'Etudes Spatiales (CNES), 52 rue Jacques Hillairet, 75612 Paris Cedex, France,
david.monchaux@cnes.fr, dominique.besson@cnes.fr
* Corresponding Author

Abstract

Being able to monitor the state of health of reusable launcher systems is a major concern. A health monitoring system (HMS) should provide a reliable information on the system's integrity and guide the maintenance process with the most accurate information possible, in the shortest possible time, with the smallest possible overhead in terms of size, weight and power consumption (SWaP).
Electrical harnesses are critical components, and several failures implying this function were already reported in launchers history. Cables and connectors are deployed through long ducts and are subject to high temperature gradients, and eventually, to chafing.
In a previous work, we presented a reflectometry system aiming to monitor the health status of the power harness of a reusable launcher. A reflectometer is able to sense impedance variations in a propagation channel which can be due to several causes such as an intermittent fault in the harness causing a short/open circuit, soft defect due to harsh environmental conditions, but it can also be caused by normal changes within the system, for example during high current peaks.
The monitoring system should be as sensitive as possible, but with as few false alarms as possible. This study's goal is to ensure that the presence of batteries will not cause false alarms in the system especially during power consumption peaks. In a first part, we give details about the mission, and more specifically about the power harness. The use case is completed by the description of a representative battery pack suitable for such a mission.
Then, we characterize the representative battery pack, exploring the following parameters: the remaining energy and the instantaneous current. For that, we realized a dedicated measurement bench to extract the complex impedance of the battery when delivering a specific current.
Then, in a third part, we inject the battery model, characterized by its complex impedance, in the model of harness, and simulate reflectometry measurements on it. The influence of current peaks is brought to light by comparing different simulations where the instantaneous current goes up, while other parameters are left unchanged.
Finally, we conclude on the sensitivity of our harness monitoring systems in the presence of power consumption peaks.

Keywords: Battery, health monitoring, modeling, reflectometry, electrical harness, reusable launcher

Acronyms/Abbreviations
HMS: Health Monitoring System
RLV: Reusable Launch Vehicle
SOC: State Of Charge
VNA: Vector Network Analyser
PCB: Printed Circuit Board
ADC: Analog-to-Digital Converter
DAC: Digital-to-Analog Converter

1. Introduction

The transition to the use of Reusable Launch Vehicles comes with new issues namely that of maintenance. Preventive maintenance is the solution to ensure reliable and safe reuse of the system. In particular, harsh environmental stressors of the space launch such as mechanical, heat, vibration etc. contribute to accelerated degradation of the cables which can result to severe damages and affect the overall functionality of the system. In a previous work [1], we proposed the main guidelines of a Health Monitoring System (HMS) able to assess the structural state of wires in a Reusable Launch Vehicle (RLV). The proposed system included two reflectometers able to monitor progressive degradations and intermittent faults on the harness network. These sensors are based on the principle that waves are partially or completely reflected at impedance changes along the path.
On the other hand, the power harness includes one or several batteries that provides the power to all systems. Depending on the mission, the batteries are likely to supply highly fluctuating currents, notably when powering flight control actuators.

Quick current variations may cause impedance fluctuations in the batteries, which could confuse the reflectometers because these disturbances would look like transient faults in wires. Then, in order to avoid false alarms, the sensitivity should be lowered so much that the system could not properly fulfill its mission of detecting intermittent wire defects.

The work presented here consists in quantifying the effects of the batteries in the reflectometry captures, in various realistic states, considering the actual mission. The main challenge was to obtain an accurate model of the batteries to use in our reflectometry simulations. For that purpose, an important step of this work consisted of sizing the battery pack that could be used in the mission. Then battery modelling was investigated in a high frequency range.

This paper is organised as follows. In Section 2, we make a brief review of the reflectometry system proposed so far in [1] to monitor the health status of the power harness. In Section 3, we give details about the context of the study. In Section 4, we characterize the representative battery pack and describe the developed measurement bench used to extract the complex impedance of the battery when delivering a specific current. Section 5 reports reflectometry measurements taking into account battery effect. Finally, concluding remarks are drawn in Section 6.

2. Principle of reflectometry

Reflectometry is a well-known technique that has been widely used to detect faults in electrical systems [2,3,4].

First, a reflectometer is a device that aims at characterizing a propagation medium. This medium can be a pair of wires, on which electric signals can propagate. Second, a reflectometer embeds a signal generation process, which can inject a deterministic and arbitrary signal (current from a current source, for example) at one or several injection points of the propagation medium. Third, a reflectometer embeds a signal acquisition process, which can capture signals (voltage, for example) at one or several capture points of the propagation medium. Finally, a reflectometer includes some signal processing that gives an estimation of the medium, by confronting the captured signal with the deterministic injected signal. Usually, we tend to use the term “reflectometry” when the injection points are at the same places than the capture points, otherwise we rather use the term “transferometry”.

Practically, reflectometers for cable diagnosis are able to spot impedance discontinuities in a cable. These discontinuities can have different causes such as topographic particularities (branches), the presence of loads, or defects on the cable. For example, in Fig. 1, a reflectometer is described, connected on its cable network under test. This cable network is made of several cable sections, one junction, and at both extremities two loads (actually two open circuits).

The reflectometer is able to produce a “reflectogram”, which is the impulsional response of the network, that is the response of the system to a short pulse. The reflectogram in Fig. 2 corresponds to the setup in Fig. 1. Several peaks are visible in it, which materialize the main features of the network, the branch separation, the two open extremities, etc.

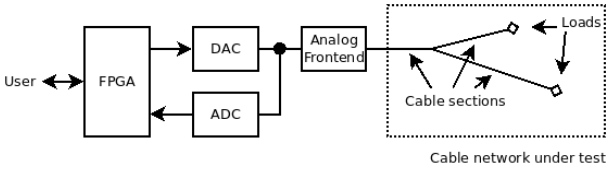

Fig. 1. Example of a reflectometer connected to a cable network under test

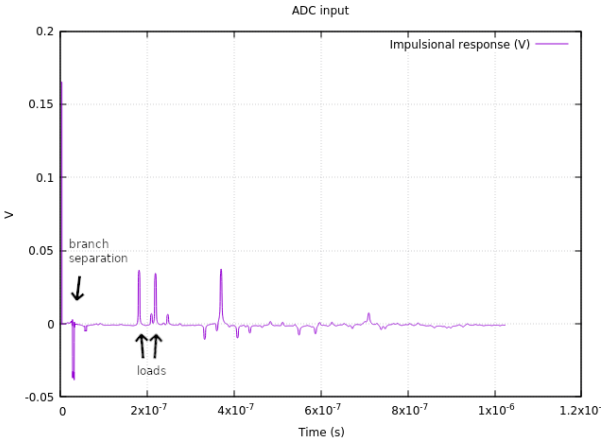

Fig. 2. Reflectogram corresponding to the schematic of Fig. 1.

2.B: problematics

In the objective of harness monitoring in RLV, the reflectometry monitoring system that we designed is supposed to make on-line measurements throughout one or several missions. When doing so, it is able to detect progressive degradations in time, but it is also able to monitor intermittent faults occurring on the harness for various reasons. For example, we can think of a loose contact in a connector, which can impair the function of the whole system, but which would fail only under mechanical vibrations. This kind of fault may be difficult to track. Reflectometry can be for that case a well-suited tool, due to its short capture periodicity, down to 10µs. However, to enhance the chances of detection, we use baselining methods, comparing current state of measurements to a well-defined reference, which renders it more sensible to small variations of the propagation media.

In the previous work [1], we considered a simple model for the batteries, based on the work of [5]. Basically, the batteries could be replaced by a current source with a

very low complex output impedance. For the reflectometry, it looks very much like a localized short-circuit. That approximate "short circuit" model we used then was static, and did not take into account any variation of the state of the batteries, neither the SOC nor the existence of sudden surge of current.
Therefore, it exists a risk that these changes would show on reflectometry measurements and be confused with intermittent faults detection. It became necessary to assess this impact with an experiment-based new model for the batteries.

3. Description of the mission – battery pack dimensioning

Our main goal is to equip the power harness of a RLV with a wire monitoring system. The harness is made of two parts, one at the top and one at the bottom, but these two parts are connected together. There is one battery pack in the top part and another one in the bottom part. One typical mission can be divided into 3 phases: pre-flight, flight, and post-flight. The battery usage are different for all flight phases. For example, Table 1 summarizes the battery needs for the top battery pack in our use case.

Table 1. Battery needs for the top battery pack

Flight phase	Duration	Power	Energy
Pre-flight	90 s	Constant: 450 W	11 Wh
Flight	300 s	Constant: 450 W	Min: 38 Wh
		+ Peaks: 2000 W	Max: 208 Wh
Post-flight	3600 s	Constant: 250 W	250 Wh

These phase-dependent needs allow sketching a more precise picture of the top battery pack given in Table 2.

Table 2. Battery needs for the top battery pack

Nominal voltage	28 V
Mass	< 12 kg
Energy	≥ 560 Wh
Power during flight phase (low)	450 W
Power during flight phase (high)	2500 W

In our study, we proposed to realize this battery pack by combining several LG INR18650HG2 battery cells. An assembly of 8 cells in series and 9 cells in parallel allows to satisfy the mission constraints as can be shown in Table 3.

So, we make the hypothesis that during the flight phase, the current drain of every individual cell of the pack can alternate between 1.7 A (normal) and 9.6 A (peak).

Table 3. Top battery pack characteristics for a 8-series/9-parallel assembly of LG INR18650HG2 cells

Nominal voltage	28,8 V
Energy	587 Wh
Max power	5054 W
Min. current per cell during flight phase	1.7 A
Max. current per cell during flight phase	9.6 A
Total mass (including overhead assembly of +40 %)	4,7 kg

4. Battery characterization

In this work, we characterize the battery pack with its complex impedance as it can be easily injected in our reflectometry simulations. It was deduced from the impedance of a single battery cell considering different operating scenarios and for different SOC.
Impedance measurement of battery cells has been deeply investigated in literature. Impedance spectroscopy (Electrochemical Impedance Spectroscopy) is a widely used technique to fully and non-destructively characterize this impedance. However, it is limited to low frequency range from a few µHz to a few kHz [6]. Battery modelling at high frequency is not well established in the literature yet. Very recent studies [7,8] have shown that at high frequency batteries show an inductive behaviour where their low frequency behaviour is capacitive. In [7], the authors propose a new method to determine the electrochemical impedance of the battery over a frequency range from 1 kHz to 300 MHz. In this section, we describe the methodology used to accurately estimate the impedance of the battery cell.

4.1. Measurement Setup

The battery cell impedance was inferred from the Scattering parameters (S-parameters) obtained using a Vector Network Analyser (VNA) connected to the battery cell, over a frequency range from 9 KHz to 3 GHz. A printed circuit board (PCB) was designed to properly connect the cell battery to the VNA, as shown in Fig. 3(a). The aim of the test board was to provide an environment to the cell to measure it while it was in a specific discharge situation. The electrical schematic of this board is shown in Fig. 3(b). Two values of the resistor *R* were considered to investigate two different operating scenarios: a slow and a fast discharge. Moreover, the impedance measurements were performed for different SOC of the cell battery. To measure the SOC of the cell battery during the test, we employed the Coulomb counting method where we mathematically integrate the current readings over the usage period.

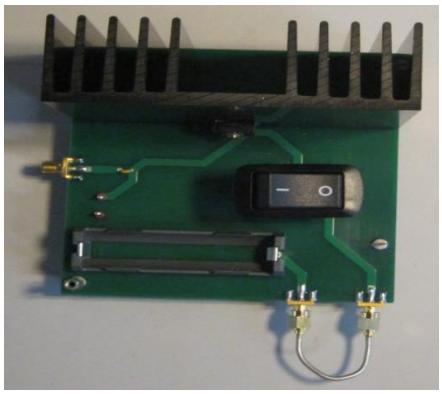

(a)

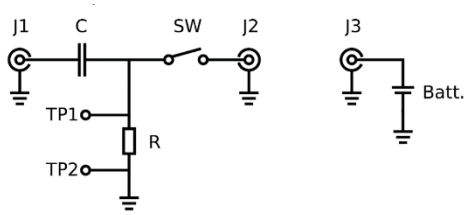

(b)

Fig. 3. (a) PCB test fixture (b) electrical schematic.

4.2. De-embedding procedure

A de-embedding process was applied to remove the effect of the PCB fixture from the impedance measurement. It relies on three steps. First, a single port measurement is performed on the battery cell and the PCB fixture together, by simply connecting the connector J2 to J3 and the connector J1 to the VNA (see Fig. 3(b)). The corresponding characteristic impedance is as follows:

$$Z^{C+B} = Z_1 \frac{1+S_{11}^{C+B}}{1-S_{11}^{C+B}} \quad (1)$$

Where, Z_1 corresponds to the VNA's test port impedance and $S_{11}{}^{C+B}$ is the 1-port reflection coefficient of the network.

The second step consists in performing a 2-port S-parameter measurement of the PCB fixture without the battery cell by connecting the J_1 and J_2 connector to the port 1 and 2 of the VNA, respectively. The obtained matrix values given in (2), describes the transmission and reflection behaviour of the PCB fixture.

$$\begin{pmatrix} S^C{}_{11} & S^C{}_{12} \\ S^C{}_{21} & S^C{}_{22} \end{pmatrix} \quad (2)$$

In the third step, we virtually close the 2-port network with the unknown impedance of the battery (Z_{batt}) as shown in Fig. 4, which is equivalent to the 1-port network measured in the first step.

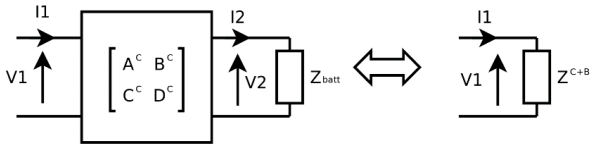

Fig. 4. 2-port network virtually closed with the unknown impedance of the cell battery.

Where, $\begin{bmatrix} A^C & B^C \\ C^C & D^C \end{bmatrix}$ are the values obtained from the conversion of the S-parameter matrix in Eq to ABCD matrix. With this description, we can express the relationship of the input voltage and current to the output voltage and current as follows:

$$\begin{cases} V_1 = A^C V_2 + B^C I_2 \\ I_1 = C^C V_2 + D^C I_2 \end{cases} \quad (3)$$

With the presence of the load Z_{batt} in the port 2, we get the following equation:

$$Z_{batt} = \frac{V_2}{I_2} \quad (4)$$

And with the 1-port network consisting of the PCB fixture plus the battery together, we can write:

$$Z^{C+B} = \frac{V_1}{I_1} \quad (5)$$

After calculations, we obtain the following equation of the de-embedded battery cell complex impedance:

$$Z_{batt} = \frac{B^C - D^C Z^{C+B}}{C^C Z^{C+B} - A^C} \quad (6)$$

5. Simulation results

Fig. 5 shows a typical topology of the harness of our use case [1].

Two reflectometer sensors have been added allowing the monitoring of the whole network.

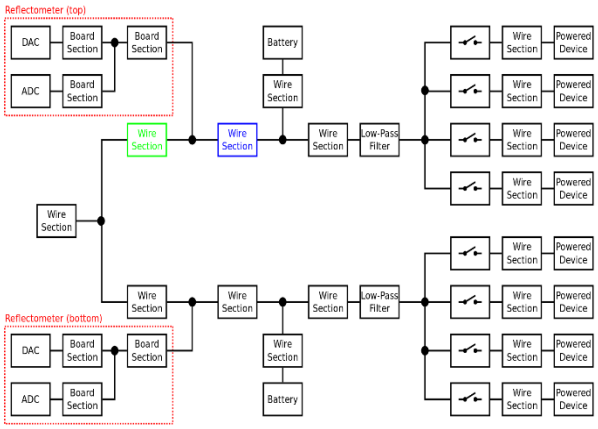

Fig. 5. Topology used for simulation[1].

The network was modeled and simulated using a reflectometry simulator designed within CEA. The model includes a modeling of the harness cables, analogical filters, switches and the battery pack characterized through its complex impedance as shown in the previous section.

The reflectometer sensor, including an FPGA, a DAC and an ADC, has also been modeled taking into account all the components present in the propagation path.

The simulation parameters such as the frequency of the DAC, the frequency of the ADC as well as the signal shape and samples were chosen to satisfy the constraints of a monitoring system in adequation with the defects to detect (spatial and time resolution, etc.).

In order to observe the effect of an instantaneous peak current disturbing the reflectometry measurements, we simulated the network for different SOC of the battery considering the two operating modes (slow and fast discharge). We considered that the two batteries present in the upper and lower branch of the network undergo the same discharge and the same current draw. Consequently, their impedances are always the same. In what follows, all the figures correspond to the simulation results of the reflectometer present in the lower part, unless otherwise specified.

Fig. 6 shows the reflectograms for different SOC (ranging from 99% to 10%) for slow and fast operating modes. We notice that there is almost no impact of the SOC of variation on the reflectograms curves for both operating scenarios.

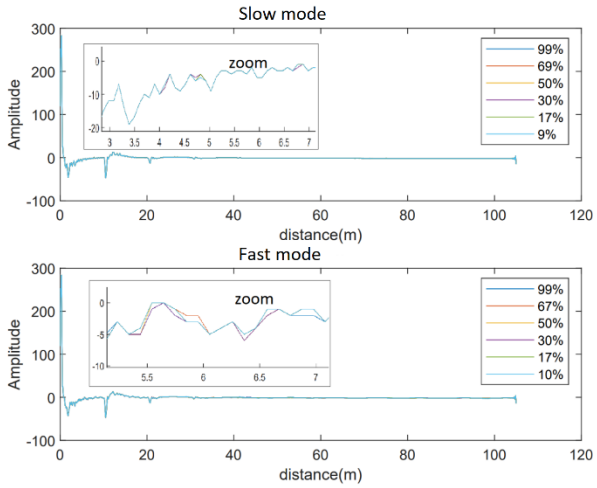

Fig. 6. Effect of the battery SOC on the reflectograms.

To simulate the effect of an instantaneous peak current on the reflectogram, we had considered that the slow mode is the reference operating mode of the batteries and that the fast mode occurs when there is a more powerful current request. Obviously, the comparison has been performed for the same SOC of the batteries.

Two cases were considered: first, when only one battery (upper or lower) encounters a consumption peak demand and second when both batteries make an instantaneous current peak at the same time.

Fig. 7 shows the differential reflectogram, which is the difference between a reference reflectogram obtained in a normal (slow) operating mode and the measured reflectogram by the two reflectometer sensors for different SOC in the case where both batteries operates in the fast operating mode.

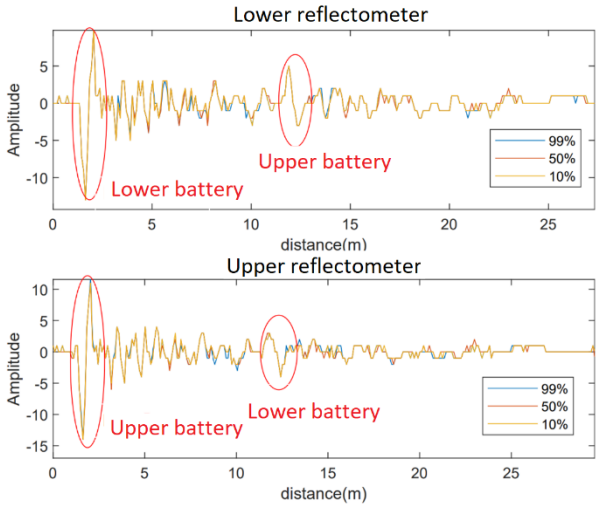

Fig. 7. Effect of an instantaneous current peak supply by both batteries on the differential reflectogram. The amplitude scale corresponds to the ADC output scale.

Fig. 8 shows the impact of an instantaneous current peak on the upper battery observed by the two reflectometers. We observe a signature corresponding to the instantaneous peak current. The location of this signature depends on the distance between the reflectometer sensor and the battery delivering the current. Nevertheless, the amplitude of the peak signature has the same order of magnitude than the noise present during the test. Thus, the effect of the current peak cannot be confused with a soft fault. Note however that the tests were made with un-aged batteries. The impact could be more important in case of aged ones.

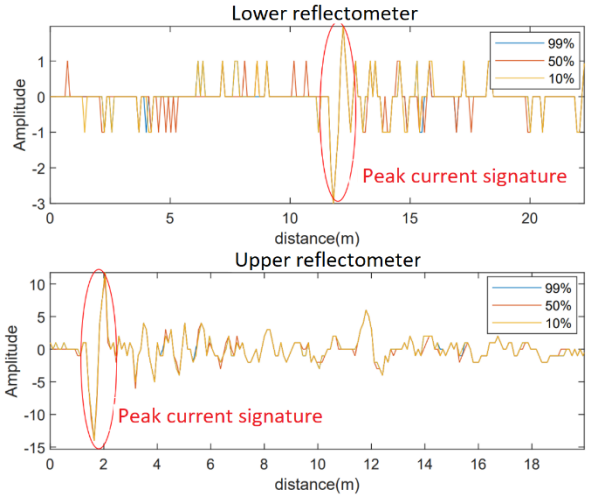

Fig. 8. Effect of an instantaneous current peak request from the upper battery on the differential reflectogram.

6. Conclusions

In this work, we have investigated whether the presence of batteries on the power harness could interfere with reflectometry measurements. An experimental setup to extract an accurate model of the battery pack was conducted applying a de-embedding process in order to remove the effect of the PCB test fixture. The quantification of the disturbance caused by the batteries was estimated by gathering measurement data for various load configurations and different SOC of the battery. Reflectometry simulations were performed on a representative power harness including the new battery model. Results show that the impact of batteries remain quite invisible especially in a noisy environment such as a RLV, at least the noise introduced due to batteries will be masked by other noise sources.

References

[1] N. Grégis, M. Cartron, and D. Monchaux. 2019. A New Design of an Embedded System for Online Harness Monitoring in Reusable Launch Vehicles Using Reflectometry. 8th European Conference for Aeronautics and Space Sciences (EUCASS).

[2] Cynthia M. Furse, Moussa Kafal, Reza Razzaghi and Yong-June Shin. Fault Diagnosis for Electrical Systems and Power Networks: A Review. IEEE SENSORS JOURNAL, VOL. 21, NO. 2, JANUARY 15, 2021

[3] E. Cabanillas, M. Kafal, and W. Ben-Hassen, “On the implementation of embedded communication over reflectometry-oriented hardware for distributed diagnosis in complex wiring networks,” in Proc. IEEE AUTOTESTCON, Sep. 2018, pp. 1–6.

[4] W. B. Hassen, F. Auzanneau, L. Incarbone, F. Peres, and A. P. Tchangani, “Distributed sensor fusion for wire fault location using sensor clustering strategy,” Int. J. Distrib. Sensor Netw., Jan. 2015. Accessed: Dec. 4, 2019.

[5] Narula A..2012. Modeling of Ageing of Lithium-Ion Battery at Low Temperatures. Master of Science Thesis. Chalmers University of Technology, Department of Energy and Environment.

[6] E. Barsoukov and J. R. Macdonald, Eds., Impedance Spectroscopy: Theory, Experiment, and Applications. Hoboken, New Jersey: John Wiley & Sons, Inc., 2005.

[7] T. Landinger et al. A Novel Method for High Frequency Battery Impedance Measurements. 2019 IEEE International Symposium on Electromagnetic Compatibility (EMC).

[8] Thomas F. Landinger et al. High frequency impedance characteristics of cylindrical lithium-ion cells: Physical-based modeling of cell state and cell design dependencies. 2021 Journal of Power sources